Optical subharmonic Rabi resonances

Stephanos Papademetriou, Stephen Chakmakjian,* and C. R. Stroud, Jr.

The Institute of Optics, University of Rochester, Rochester, New York 14627

Received September 9, 1991

We report the observation of the first six subharmonic resonances of the Rabi frequency in the absorption of a 100% amplitude-modulated laser beam by a two-level atom. The amplitude-modulated field is formed by combining two separate cw lasers; one is held fixed in frequency, and the other, of equal amplitude, is scanned in frequency. We present data and theory for several values of the detuning between the fixed field and the atomic resonance. The experimental results are in good agreement with theory.

1. INTRODUCTION

The interaction of a strong bichromatic field with a two-level atomic transition is fundamental to a number of research disciplines, including nonlinear optics, quantum optics, and laser theory. When the two field components are mutually coherent, we may equivalently describe the field as being 100% amplitude modulated (AM). The atomic variables exhibit resonant behavior when the modulation frequency is approximately equal to the Rabi frequency or any subharmonic of the Rabi frequency. There have been numerous theoretical and experimental studies of the interaction of both single-mode fields and strongly modulated multimode fields with two-level atoms.[1-16] Here we present the results of an experiment using a new technique to study the absorption of a field that is 100% AM by a two-level atom. In this technique the Rabi frequency is held fixed and the modulation frequency is varied. This method provides much better resolution of the higher subharmonic resonances than does the conventional technique of keeping the modulation frequency fixed and varying the Rabi frequency.

These subharmonic resonances show up in other contexts. Agarwal showed that they occur in the Raman effect[17] and that the generation of squeezed states of the phase of the field is possible in multiwave mixing at the subharmonic Rabi resonances.[18] The interaction of strong bichromatic fields with atomic media has also been related to various laser instabilities. Hillman *et al.*[19,20] and Stroud *et al.*[21] found that a dye laser operating at more than 1.5 times above threshold is unstable for single-frequency operation and will switch to bichromatic operation. Feldman and Feld[7] showed that single-mode gas lasers exhibit the subharmonic structure mentioned above, which is indicative of the presence of a bichromatic field. These subharmonic resonances may also provide the necessary mechanism that induces the period-doubling bifurcations and the eventual chaotic behavior that has been observed in inhomogeneously broadened lasers.[8] Similar effects were observed in rf spectroscopy. Bonch-Bruevich *et al.*[9] used two strong rf fields tuned to a Zeeman resonance in cadmium. Spontaneous emission that is important to optical-frequency experiments is effectively absent in rf spectroscopy. The method used in the Bonch-Bruevich experiment is the rf analog of that used in the current optical experiment.

2. THEORY

The experiment was performed by keeping one strong field fixed in frequency while another field of equal amplitude was tuned. Although there have been a number of publications of theories of the interaction of a bichromatic field with a two-level atom, none has been carried out in a framework appropriate to describe this experimental situation. We quickly review the theory in a form appropriate for our present needs.

The fields in this experiment were circularly polarized and coupled only two particular hyperfine levels. Because only these two levels were involved, polarization properties were not important in the dynamics, and we can write the total field $\mathcal{E}$ in the scalar form

$$\mathcal{E}(t) = 2E_1 \cos(\omega_1 t) + 2E_2 \cos[(\omega_1 + \delta\omega)t + \theta]. \quad (1)$$

Here the amplitudes of the fixed and tuned fields are E_1 and E_2, respectively. The phase between the oscillations of the two fields at time $t = 0$ is θ. The beat frequency between the two optical fields is $\delta\omega$, which is twice the modulation frequency of the 100%-AM field described by Eq. (1). Simple trigonometric manipulations allow us to write Eq. (1) as

$$\mathcal{E}(t) = 2E'(t)\cos\omega_1 t - 2E''(t)\sin\omega_1 t, \quad (2)$$

where

$$E'(t) = E_1 + E_2 \cos(\delta\omega t + \theta), \quad (3)$$

$$E''(t) = E_2 \sin(\delta\omega t + \theta). \quad (4)$$

The components of the total electric field that are in phase and in quadrature to a frame rotating at the frequency of the fixed field at frequency ω_1 are $E'(t)$ and $E''(t)$, respectively.

The optical Bloch equations model the response of a two-level atom coherently driven by an optical field.[22] In the rotating frame of the red-shifted laser ω_1, the optical Bloch equations are

$$\frac{d}{dt}\begin{bmatrix} u \\ v \\ w \end{bmatrix} = \begin{bmatrix} -1/T_2 & -\Delta & -\kappa E''(t) \\ \Delta & -1/T_2 & \kappa E'(t) \\ \kappa E''(t) & -\kappa E'(t) & -1/T_1 \end{bmatrix}\begin{bmatrix} u \\ v \\ w \end{bmatrix} + \begin{bmatrix} 0 \\ 0 \\ w_{eq}/T_1 \end{bmatrix}, \quad (5)$$

0740-3224/92/071182-07$05.00

in which

$$\Delta = \omega_0 - \omega_1, \tag{6a}$$

$$\kappa = 2d/\hbar. \tag{6b}$$

The frequency difference between the two atomic levels is ω_0, while the dipole-moment matrix element between them is d. The detuning of the fixed field from atomic resonance is denoted by Δ. The relaxation times of the atomic inversion and polarization are T_1 and T_2, respectively. The slowly varying amplitude of the in-phase and in-quadrature parts of the dipole moment are u and v, respectively. The inversion of the two-level atom is w, and w_{eq} is the value to which the inversion decays in the absence of a field. The coefficients in the system of differential equations in Eq. (5) are periodic in time. According to Floquet's theorem[23] the stationary-state solution can be expanded as a Fourier series in terms of the fundamental frequency of the system. In other words, the stationary-state solution can be written as

$$\begin{bmatrix} u(t) \\ v(t) \\ w(t) \end{bmatrix} = \sum_{n=-\infty}^{\infty} \begin{bmatrix} u_n \\ v_n \\ w_n \end{bmatrix} \exp(in\delta\omega t). \tag{7}$$

By substituting Eq. (7) into Eq. (5), we obtain the following recurrence relations:

$$(1 + in\delta\omega T_2)u_n + \Delta T_2 v_n - (i/2)\Omega_2 T_2 w_{n-1} + (i/2)\Omega_2^* T_2 w_{n+1} = 0, \tag{8a}$$

$$(1 + in\delta\omega T_2)v_n - \Delta T_2 u_n - \Omega_1 T_2 w_n - \tfrac{1}{2}\Omega_2 T_2 w_{n-1} - \tfrac{1}{2}\Omega_2^* T_2 w_{n+1} = 0, \tag{8b}$$

$$(1 + in\delta\omega T_1)w_n + i/2\Omega_2 T_1 u_{n-1} - (i/2)\Omega_2^* T_1 u_{n+1} + \Omega_1 T_1 v_n + \tfrac{1}{2}\Omega_2 T_1 v_{n-1} + \tfrac{1}{2}\Omega_2^* T_1 v_{n+1} = w_{eq}\delta_{n,0}, \tag{8c}$$

in which

$$\Omega_1 = \kappa E_1, \tag{9a}$$

$$\Omega_2 = \kappa E_2 \exp(i\theta) \tag{9b}$$

are the Rabi frequencies of the two fields, and the asterisk denotes a complex conjugate. The Kronecker δ function is $\delta_{n,0}$. The above recurrence relations can be written in matrix form:

$$B_0\phi_{n-1} + A_n\phi_n + B_0^*\phi_{n+1} = D_n, \tag{10}$$

where

$$A_n = \begin{bmatrix} (1 + in\delta\omega T_2) & \Delta T_2 & 0 \\ -\Delta T_2 & (1 + in\delta\omega T_2) & -\Omega_1 T_2 \\ 0 & \Omega_1 T_1 & (1 + in\delta\omega T_1) \end{bmatrix},$$

$$B_0 = \begin{bmatrix} 0 & 0 & -(i/2)\Omega_2 T_2 \\ 0 & 0 & -\tfrac{1}{2}\Omega_2 T_2 \\ (i/2)\Omega_2 T_1 & \tfrac{1}{2}\Omega_2 T_1 & 0 \end{bmatrix},$$

$$D_n = \begin{bmatrix} 0 \\ 0 \\ w_{eq}\delta_{n,0} \end{bmatrix},$$

$$\phi_n = \begin{bmatrix} u_n \\ v_n \\ w_n \end{bmatrix}. \tag{11}$$

We solve this three-term matrix recurrence relation by using matrix continued fractions.[24,25] The details of the calculation are outlined in Appendix A. The time-averaged atomic inversion w_0 is given by the third component of the ϕ_0 vector in Eq. (A14). The absorption of the bichromatic field can be written as the time-averaged product of the electric field and the time rate of change of the polarization,

$$\left\langle \mathscr{E}(t)\frac{dP}{dt} \right\rangle_{time} = \frac{-\omega_1}{2\kappa}[\Omega_1 v_0 + \Re(v_1\Omega_2^*) + \Im(u_1\Omega_2^*)], \tag{12}$$

where the complex polarization is given by

$$P(t) = (d/2)[u(t) + iv(t)]\exp(i\omega_1 t) \tag{13}$$

and $\Re$ and $\Im$ denote the real and imaginary parts, respectively. In the time average we have first averaged over the optical period and then over a period of the beat frequency between the two optical fields. We also used the fact that $u(t)$ and $v(t)$ are real variables, and therefore their Fourier transforms are Hermitian (i.e., $u_n = u_{-n}^*$ and $v_n = v_{-n}^*$). From Eq. (8c), with $n = 0$, we get an expression for the time-averaged inversion of the atoms:

$$w_{eq} - w_0 = T_1[\Omega_1 v_0 + \Re(v_1\Omega_2^*) + \Im(u_1\Omega_2^*)]. \tag{14}$$

A comparison of Eqs. (13) and (14) shows that there is a relation between the rate of absorption by a two-level atom in the presence of a 100%-AM field and the time-averaged inversion, w_0.

In the experiment the fluorescence from the excited atoms is measured. In the steady state the rate of absorption is exactly equal to the rate of fluorescence. The rate of fluorescence is proportional to the time-averaged excited-state population, ρ_{e0}, which can be directly written in terms of w_0,

$$\rho_{e0}(\delta\omega) = [1 + w_0(\delta\omega)]/2. \tag{15}$$

We show the dependence on the beat frequency $\delta\omega$ explicity in Eq. (15) to emphasize that $\delta\omega$ is the independent quantity in our experiment. A plot of Eq. (15) is shown in Fig. 1(a). In this figure and throughout the remainder of the paper we scale the various frequencies by multiplying them by T_2. In the case of the sodium D lines the radiative damping time of the polarization is given by $T_2 = 2 \times T_1 = 33$ ns. This curve is quite complicated, and it shows several resonances in the absorption spectrum of the bichromatic field. The nature of these resonances is better understood in the symmetric problem, for which the center of the 100%-AM field is positioned on resonance with the atoms, and both fields are swept simultaneously, symmetrically about their center frequency.[11,12,20] The inversion is coherently driven to oscillate at the Rabi frequency. Maximum absorption occurs when the field is modulated at the same frequency as this oscillation. A secondary maximum occurs when the field is modulated at one half of the rate at which the inversion oscillates. Additional resonances occur at the other subharmonics of the Rabi frequency. The behavior of this interaction has been compared with that of a swing that is pushed every nth round trip[20] or of an anharmonic oscillator that is driven every nth cycle of its natural frequency.[11]

The quantity measured directly in the experiment, as is described in more detail in Section 3, is the difference be-

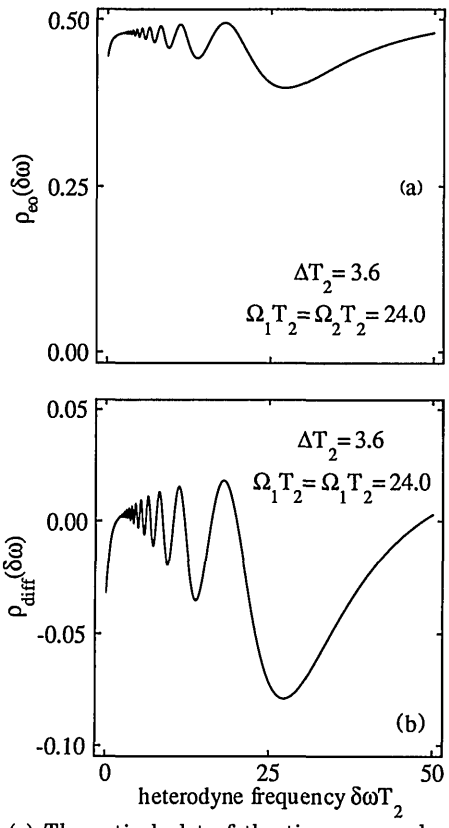

Fig. 1. (a) Theoretical plot of the time-averaged excited-state population as a function of the frequency separation $\delta\omega T_2$ between the two laser fields. The Rabi frequencies of both fields are held fixed and equal to each other and are $\Omega_1 T_2 = \Omega_2 T_2 = 24$. The fixed laser field Ω_1 is positioned 18 MHz to the red side of the atomic transition, $\Delta T_2 = 3.6$. We assume throughout that the atoms are radiatively broadened, $T_1/T_2 = 0.5$. In the sodium experiment $T_2 = 33$ ns. (b) Differential time-averaged excited-state population as a function of the frequency separation $\delta\omega T_2$ between the two laser fields. The parameters are identical to those for (a).

tween the time-averaged excited-state population in the presence of the bichromatic field, $\rho_{e0}(\delta\omega)$, and that when just the fixed field E_1 is present, ρ_e. The steady-state excited-state population of a two-level atom in the presence of a single field is easily derived from Eq. (5) by setting $E_2 = \delta\omega = \theta = 0$:

$$\rho_{e0} = \frac{I_1}{2[1 + (\Delta T_2)^2 + I_1]}, \tag{16}$$

where I_1 is the dimensionless intensity associated with the fixed field E_1 and is given by

$$I_1 = \Omega_1^2 T_1 T_2. \tag{17}$$

The signal that we measure in the laboratory is then best described by the differential quantity

$$\rho_{diff}(\delta\omega) = \rho_{e0}(\delta\omega) - \rho_{e0}. \tag{18}$$

The advantage of looking at the differential quantity $\rho_{diff}(\delta\omega)$ rather than $\rho_{e0}(\delta\omega)$ of Eq. (16) becomes obvious in a comparison of Fig. 1(b), which is a plot of Eq. (18), with Fig. 1(a). The large dc signal produced by the saturation by a single field, the fixed field, has been removed in $\rho_{diff}(\delta\omega)$. Thus the differential signal can be used to zoom into the interesting resonant structure of the absorption under bichromatic excitation. This point is also discussed in Section 3 in more detail.

3. EXPERIMENTAL PROCEDURE

The 100%-AM optical field is created by interferometrically combining the output beams from two independent frequency-stabilized dye lasers. The output from one port of the beam splitter (Fig. 2) is used to excite the atoms in the sodium atomic beam, whereas the beam from the other port of the beam splitter is used for analysis. The relative intensity of the two laser beams is adjusted so that the signal produced when they are combined on a fast photodiode is 100% AM. The modulation frequency in this case is actually one half of the heterodyne difference frequency between the two lasers. The sodium atomic beam is collimated by two 0.4-mm pinholes separated by 40 cm. This arrangement of the pinholes, together with an oven temperature of 350°C, defines an atomic beam with a residual Doppler broadening of 1–2 MHz. For more details on the atomic beam setup see Refs. 11 and 12. A two-level system was obtained by pumping the population into the aligned magnetic sublevels.[26]

To obtain the response of the atoms as a function of the heterodyne frequency, we collected the fluorescence emitted from atoms excited by the bichromatic optical field. As is indicated in Section 2, the magnitude of the absorption of the bichromatic field is proportional to the time-averaged excited-state population, which itself is proportional to the time-averaged fluorescent intensity. Therefore the time-averaged fluorescent intensity is measured in order to measure the AM absorption spectrum. The collection of fluorescent emission is a signal-limited detection scheme, which is greatly preferable to measuring the small amount of absorption of light from the excitation beam.

To improve the signal-to-noise ratio further, we chopped the beam from the frequency-scanning laser at 90 kHz by

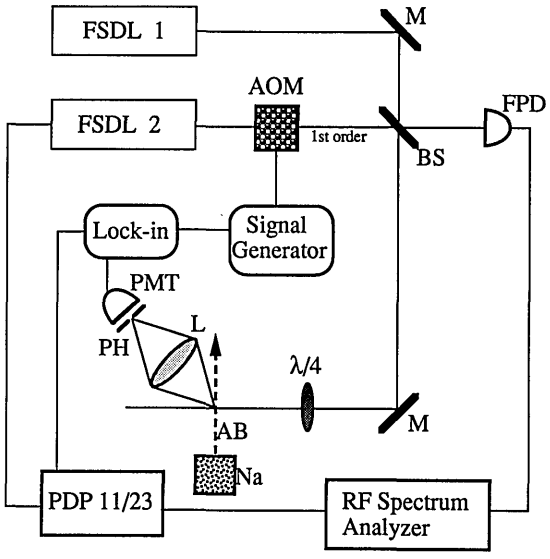

Fig. 2. Experimental apparatus. FSDL's, frequency stabilized dye lasers; AOM, acousto-optic modulator; M's, mirrors; BS, beam splitter; PH, pinhole; λ/4, quarter-wave plate; L, lens; AB, atomic beam; PMT, photomultiplier tube; FPD, fast photodiode; PDP 11/23, microcomputer.

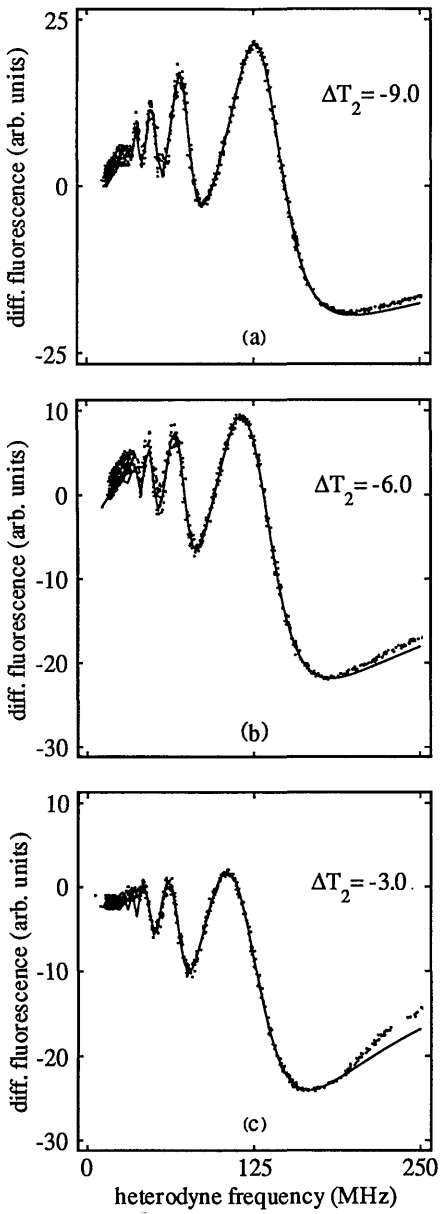

Fig. 3. Time-averaged differential lock-in signal as a function of the frequency difference between the two lasers for three different detunings of the fixed-frequency laser on the blue side of resonance. Both laser fields are of equal intensity, $\Omega_1 T_2 = \Omega_2 T_2$. (a) The fixed field, Ω_1, is positioned 45 MHz to the blue side of resonance ($\Delta T_2 = -9.0$). The best fit to the data gives, for the Rabi frequency of each field, $\Omega_1 T_2 = 23.6$. (b) The fixed field, Ω_1, is positioned 30 MHz to the blue side of resonance ($\Delta T_2 = -6.0$). The best fit to the data gives, for the Rabi frequency of each field, $\Omega_1 T_2 = 23.8$. (c) The fixed-frequency field, Ω_1, is positioned 15 MHz to the blue side of resonance ($\Delta T_2 = -3.0$). The best fit to the data gives, for the Rabi frequency of each field, $\Omega_1 T_2 = 23.8$.

using an Intra-action Model AFD 402 acousto-optic modulator driven by a Wavetek 188 signal generator. Because the chop frequency is much slower than the spontaneous decay rate for the $3\ ^2S_{1/2} \rightarrow 3\ ^2P_{3/2}$ transition in sodium, the fluorescent intensity measured by the photomultiplier adiabatically followed the amplitude modulation.

The photomultiplier signal was amplified by an optical amplification circuit capable of following the audio chop frequency but too slow to follow the rf heterodyne frequency or most of the photomultiplier tube shot noise. The resulting electrical signal was fed into the lock-in amplifier (EGG 5210). The signal out of the lock-in amplifier was proportional to the difference between the fluorescent intensity emitted from the atoms excited by the total 100%-AM field and the fluorescent intensity emitted by atoms excited by only the fixed-frequency laser. This lock-in technique eliminates the large dc portion of the signal and permits direct measurement of the signal, as is shown in Fig. 1(b).

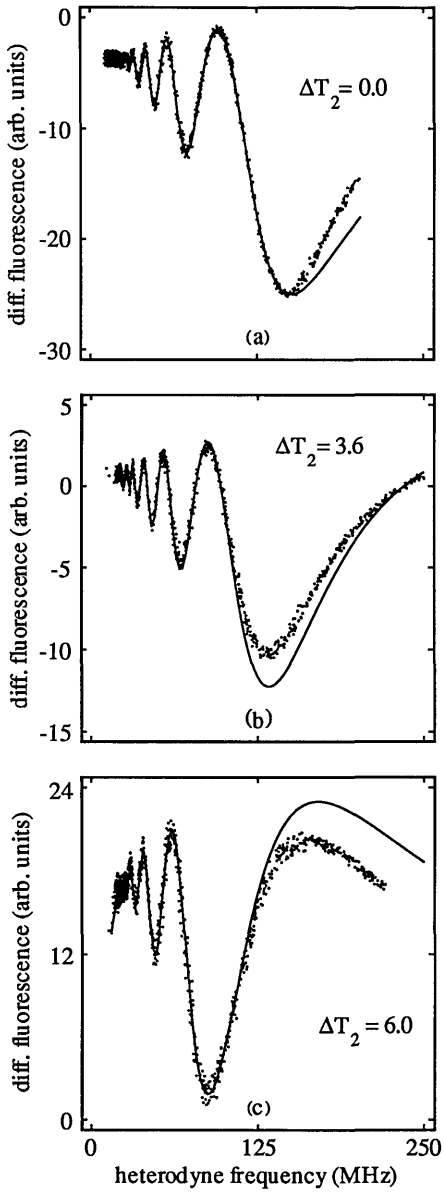

Fig. 4. (a) Time-averaged differential lock-in signal as a function of the frequency difference between the two lasers with the fixed-frequency field at resonance or tuned to the red side of resonance. The fixed-frequency field, Ω_1, is positioned on resonance with the atomic transition ($\Delta T_2 = 0.0$). The best fit to the data gives, for the Rabi frequency of each field, $\Omega_1 T_2 = 23.8$. (b) The time-averaged differential lock-in signal as a function of the frequency difference between the two lasers. Both laser fields are of equal intensity, $\Omega_1 T_2 = \Omega_2 T_2$. The fixed field, Ω_1, is positioned 18 MHz to the red side of resonance ($\Delta T_2 = 3.6$). The best fit to the data gives, for the Rabi frequency of each field, $\Omega_1 T_2 = 23.4$. (c) The fixed field, Ω_1, is positioned 30 MHz to the red side of resonance ($\Delta T_2 = 6.0$). The best fit to the data gives, for the Rabi frequency of each field, $\Omega_1 T_2 = 16.7$.

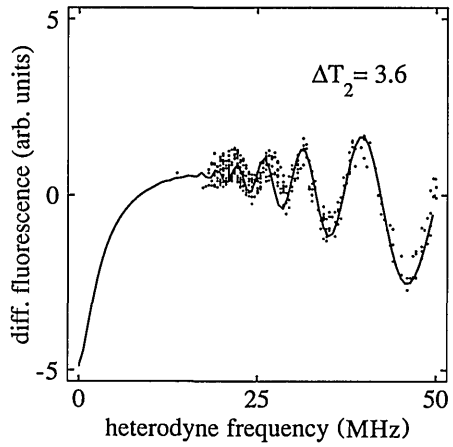

Fig. 5. Enlargement of the low-frequency detail of Fig. 4(c). One can resolve six peaks in the response of the atoms to the bichromatic field.

Two frequency-stabilized lasers are employed in these experiments. The fixed-frequency laser is a home-built laser that is locked by a closed-loop servo to a pressure-scanned, thermally stabilized confocal Fabry–Perot interferometer. This laser has less than 2-MHz excursion over 5 min. The second dye laser is a Coherent Model 699 dye laser. The operating frequency of this laser tends to drift over 5 MHz or so on a time scale of 1 min. To resolve five subharmonics, we needed to measure the modulation frequency to an accuracy of approximately 1 MHz. We were able to do this despite the drifting of the two lasers by using an rf spectrum analyzer and a transient digitizer to measure simultaneously the differential fluorescence signal from the lock-in amplifier and the heterodyne beat frequency from a photodiode illuminated by the two lasers. The drifting of the lasers then acted to scan the modulation frequency by a measured amount. The frequency range was divided into a series of bins, and the differential fluorescence value was placed into the appropriate computer bin.

For each value of fixed laser detuning a spectrum was recorded for modulation frequencies ranging from 10 to 250 MHz. The computer controlled the frequency of the scanning laser with an analog voltage. At each frequency setting of the scanning laser the computer recorded 20 realizations of the actual modulation frequency and the corresponding differential fluorescence signal measured by the lock-in detection system.

4. EXPERIMENTAL RESULTS

We collected data with the fixed field on resonance with the atomic transition and for several other values of detuning. In Figs. 3–5 we show the differential time-averaged fluorescent signal from the lock-in amplifier as a function of the heterodyne frequency difference, $\delta\omega$, between the two fields. In the same plots we also present the best theoretical fit to the data (solid curves). The theory presented in Section 2 had to be extended to take into account Doppler broadening and Gaussian beam averaging over the transverse profiles of the two laser beams.

The most significant averaging effect was found to be the residual Doppler broadening, which occurred because the combined laser fields as well as the atomic beam were not perfectly collimated at the interaction region. Also, Gaussian beam averaging was important. Both effects were easily modeled but not easily directly measured, so we used these widths as well as the fluorescence collection efficiency as fitting parameters in a simulated annealing fitting routine.

We found that the simulated annealing[27,28] is highly efficient for fitting the experimental results as shown in Figs. 3–5. By using this method, we found that the dimensionless Rabi frequency in our experiment was $\Omega T_2 = 23$ except for the case of Fig. 4 for $\Delta T_2 = 6$, for which the intensity was lowered, and the best fit to the data gave us $\Omega T_2 = 16.7$. For all six detuning cases the width of the residual Doppler broadening was $2.5T_2$, which is in excellent agreement with its expected value. The width of the intensity averaging was of the order of 20% of the mean intensity used in each case. Note that the data shown in all our plots is the raw data as taken from the lock-in amplifier. When the signal becomes positive, it means that the response of the atoms is greater for the combined field than it is for a single field.

In the case of Fig. 4(b), for $\Delta T_2 = 3.6$, the fixed field is positioned 18 MHz to the red side of atomic resonance. We obtained the best results for this detuning with regard to resolving subharmonic resonances. This is because in this case the center frequency of the resulting bichromatic field is situated close to atomic resonance for a wider range of heterodyne frequencies. The bichromatic field then interacts more strongly with the atoms, and the subharmonic structure of the atomic response becomes more prominent. At the same time the fixed field is not resonantly exciting the other two transitions in the D_2 line of sodium, which lie 60 and 95 MHz to the red of the atomic resonance.

In Fig. 5 we enlarge the scale for the data with the most structure, the detuned case with $\Delta T_2 = 3.6$. One can clearly resolve as many as six peaks in the response of the atoms. Also, the frequency binning, which is done by the spectrum analyzer as discussed in Section 3, becomes quite clear.

In Figs. 3 and 4 the higher-frequency part of the data fits better to the theory for the cases of the blue-shifted detunings than those for the red-shifted detunings. We believe that the reason is optical pumping. Our theory assumes that we have a closed two-level atomic system. The optically pumped atoms are to a good approximation two-level atoms, but there is some leakage out of the system. The leakage is larger when the fields are tuned closer to the red side of resonance, because there are competing nearby transitions on that side.

5. CONCLUSIONS

We have presented both theoretical and experimental studies of the time-averaged absorption of a 100%-AM field by a closed two-level atomic system. This is the first time to our knowledge that the absorption of a strong bichromatic field has been studied in the optical regime as a function of the modulation frequency. In our experiment we used two independent frequency-stabilized lasers. One laser was fixed in frequency, and the response of the atoms was monitored as the other laser was swept in frequency. Using a lock-in detection technique

and taking data at time scales shorter than the long-term frequency jitter of the combined laser fields enabled us to improve the frequency resolution to the point that we were able to resolve as many as six subharmonic resonances in the absorption spectrum of the two-level atoms. We also studied the absorption for different detunings between the fixed laser field and atomic resonance. Our data are in good agreement with the theoretical predictions. In calculating the theoretical best fits to our data, we have incorporated experimental complications such as intensity averaging and residual Doppler broadening.

We have demonstrated the complicated absorption structure that a bichromatic field exhibits when it interacts with a two-level atomic system. Subharmonic resonances of the Rabi frequency occur because of the coherent nonlinear interaction of the two strong fields with the atoms. We have also demonstrated a technique that provides greatly enhanced resolution in modulation spectroscopy.

APPENDIX A

In this appendix we outline the method for solving the matrix continued fraction given by Eq. (10). Furthermore, we show that the time-averaged atomic quantities (u_0,v_0,w_0) are independent of the phase difference θ between the two fields [see Eq. (1)].

By multiplying both sides of Eq. (10) by $(A_n)^{-1}$ from the left-hand side, we obtain

$$C_n\phi_{n-1} + \phi_n + G_n\phi_{n+1} = b_n, \tag{A1}$$

where

$$C_n = A_n{}^{-1}B_0, \tag{A2}$$

$$G_n = A_n{}^{-1}B_0{}^*, \tag{A3}$$

$$b_n = A_n{}^{-1}D_n. \tag{A4}$$

The main assumption for obtaining a solution to Eq. (A1) is the truncation of the infinite system at a very large index n; i.e., we set $\phi_n = 0$ for $n \geq N$. The procedure then consists of the iterative elimination of ϕ_n, ϕ_{n-1}, and so on. Practically, N must be chosen to be so large that the ϕ_n of interest are independent of the truncation index N. This assumption makes sense, since the higher-order components of ϕ_n must become less significant if the Fourier series in Eqs. (7) are to converge and the rotating-wave approximation is to remain valid.

Under this assumption the recurrence relation, Eq. (A1), for $n = N$ can be written as

$$C_N\phi_{N-1} + \phi_N = 0, \tag{A5}$$

and after solving for ϕ_N we obtain

$$\phi_N = -C_N\phi_{N-1}. \tag{A6}$$

Similarly, for $n = N - 1$, Eq. (A1) becomes

$$C_{N-1}\phi_{N-2} + \phi_{N-1} + G_{N-1}\phi_N = 0. \tag{A7}$$

Solving the above equation for ϕ_{N-1} and substituting for ϕ_N from Eq. (A6), we get

$$\phi_{N-1} = -(I - G_{N-1}C_N)^{-1}C_{N-1}\phi_{N-2}, \tag{A8}$$

where I stands for the 3×3 identity matrix. If we continue this iterative method in a similar fashion until we reach the relation for $n = 1$, we get

$$\phi_1 = -(I - G_1\{I - G_2[\ldots G_{N-2} \times (I - G_{N-1}C_N)^{-1}C_{N-1}\ldots]^{-1}C_3\}^{-1}C_2)^{-1}C_1\phi_0. \tag{A9}$$

By identifying everything to the left of ϕ_0 in the above equation as M^+, we can write Eq. (A9) as

$$\phi_1 = M^+\phi_0. \tag{A10}$$

Repeating the same procedure, starting with $n = -N$, until we reach $n = -1$, we get

$$\phi_{-1} = -(I - C_{-1}\{I - C_{-2}[\ldots C_{-N+2} \times (I - C_{-N+1}G_N)^{-1}G_{-N+1}\ldots]^{-1}G_3\}^{-1}G_{-2})^{-1}G_{-1}\phi_0. \tag{A11}$$

Again we can identify everything to the left of ϕ_0 in Eq. (A8) as M^- and write

$$\phi_{-1} = M^-\phi_0. \tag{A12}$$

Now, for $n = 0$, Eq. (A1) gives us

$$C_0\phi_{-1} + \phi_0 + G_0\phi_1 = b_0. \tag{A13}$$

With the help of Eqs. (A10) and (A12), we can now solve Eq. (10) for ϕ_0 and obtain

$$\phi_0 = (C_0M^- + G_0M^+ + I)^{-1}b_0. \tag{A14}$$

The time-averaged response of the inversion, w_0, in the presence of a strong bichromatic field is then given by the third component of the ϕ_0 vector in Eq. (A14).

To show that the time-averaged atomic quantities (u_0,v_0,w_0) are independent of the phase difference θ between the two fields, we must go back to Eq. (A1) and trace the θ dependence of the various terms. By inspection of Eq. (11), we see that only the matrix B_0 depends on θ. In particular, we can write

$$C_n = \exp(i\theta)A_n{}^{-1}B_0{}' = \exp(i\theta)C_n{}', \tag{A15}$$

$$G_n = \exp(-i\theta)A_n{}^{-1}B_0{}'{}^* = \exp(-i\theta)G_n{}', \tag{A16}$$

where $C_n{}'$ and $G_n{}'$ do not depend on θ. Now that the θ dependence is more apparent, we can see how the complex exponential terms will cancel out in Eqs. (A9) and (A11), to give

$$M^+ = \exp(i\theta)M'^+, \tag{A17}$$

$$M^- = \exp(-i\theta)M'^-, \tag{A18}$$

where again the primed quantities are independent of θ.

Using Eqs. (A15)–(A18) in Eq. (A14), we obtain

$$\phi_0 = (C_0{}'M'^- + G_0{}'M'^+ + I)^{-1}b_0. \tag{A19}$$

Because ϕ_0 does not depend on θ, we set $\theta = 0$ in all the numerical calculations of this work.

ACKNOWLEDGMENTS

We acknowledge useful discussions with Karl Koch and John Yeazell and the support of the University Research Initiative through the U.S. Army Research Office.

*Present address, Nonlinear Optics Center of Technology, Phillips Laboratory/LITN, Kirtland Air Force Base, New Mexico 87117.

REFERENCES

1. R. P. Hackel and S. Ezekiel, "Interaction of two resonant laser fields with a folded Doppler broadened system of I_2," in *Laser Spectroscopy IV,* H. Walther and K. W. Roth, eds. (Springer-Verlag, Berlin, 1979), pp. 88–95.
2. B. R. Mollow, "Stimulated emission and absorption near resonance for driven systems," Phys. Rev. A **5,** 2217–2222 (1972).
3. S. Haroche and F. Hartman, "Theory of saturated absorption line shapes," Phys. Rev. A **6,** 1280–1300 (1972).
4. F. Y. Wu, S. Ezekiel, M. Ducloy, and B. R. Mollow, "Observation of amplification in a strongly driven two-level atomic system at optical frequencies," Phys. Rev. Lett. **38,** 1077–1080 (1977).
5. M. T. Gruneisen, K. R. MacDonald, and R. W. Boyd, "Induced gain and modified absorption of a weak probe beam," J. Opt. Soc. Am. B **5,** 123–129 (1988).
6. G. I. Toptygina and E. E. Fradkin, "Theory of subradiative absorption in the interaction between two intense waves in a nonlinear medium," Sov. Phys. JETP **55,** 246–251 (1982); A. A. Mak, S. G. Przhibel'skii, and N. A. Chigir, "Nonlinear resonance phenomena in bichromatic fields," Izv. Akad. Nauk SSSR **47,** 1976–1983 (1983); G. S. Agarwal and N. Nayak, "Multiphoton processes in two-level atoms in two intense pump beams," J. Opt. Soc. Am. B **1,** 164–169 (1984).
7. B. J. Feldman and M. S. Feld, "Theory of high-intensity gas lasers," Phys. Rev. A **1,** 1375–1396 (1970).
8. R. S. Gioggia, and N. B. Abraham, Phys. Rev. Lett. **51,** 650–653 (1983); Phys. Rev. A **29,** 1304–1309 (1984).
9. A. M. Bonch-Bruevich, T. A. Vartanyan, and N. A. Chigir, "Subradiative structure in the absorption spectrum of a two-level system in a biharmonic radiation field," Sov. Phys. JETP **50,** 1070–1073 (1979).
10. P. Thomann, "Optical resonances in strong modulated laser beams," J. Phys. B **13,** 1111–1124 (1980).
11. S. Chakmakjian, K. Koch, and C. R. Stroud, Jr., "Observation of resonances at subharmonics of the Rabi frequency in the saturated absorption of a 100% amplitude-modulated laser beam," J. Opt. Soc. Am. B **5,** 2015–2020 (1988).
12. S. H. Chakmakjian, "Nonlinear optical systems interacting with amplitude-modulated optical fields," Ph.d. Dissertation (University of Rochester, Rochester, N.Y., 1990).
13. W. M. Ruyten, "Subharmonic resonances in terms of multiphoton processes and generalized Bloch–Siegert shifts," J. Opt. Soc. Am. B **6,** 1796–1802 (1989).
14. W. M. Ruyten, "Harmonic behavior of the multiphoton quantum resonances of a two-level atom driven by a fully-amplitude-modulated field," Phys. Rev. A **40,** 1447–1455 (1989); W. M. Ruyten, "Multiphoton resonances in the modulated fluorescence from an inhomogeneously broadened medium," Opt. Lett. **14,** 506–508 (1989).
15. R. E. Silverans, G. Borghs, P. De Bisschop, and M. Van Hove, "Phase effects in bichromatic field interactions with two-level atoms," Phys. Rev. Lett. **55,** 1070–1073 (1985).
16. J. H. Eberly, and V. D. Popov, "Phase dependent pump-probe line-shape formulas," Phys. Rev. A **37,** 2012–2016 (1988).
17. G. S. Agarwal, "Subharmonic Raman effect in nonlinear mixing," J. Opt. Soc. Am. B **13,** 482–484 (1988).
18. G. S. Agarwal, "Generation of squeezed states of radiation at submultiple Rabi resonances," J. Opt. Soc. Am. B **5,** 180–183 (1988).
19. L. W. Hillman, J. Krasinski, R. W. Boyd, and C. R. Stroud, Jr., "Observation of higher order dynamical states of a homogeneously broadened laser," Phys. Rev. Lett. **52,** 1605–1608 (1985).
20. L. W. Hillman, J. Krasinski, K. Koch, and C. R. Stroud, Jr., "Dynamics of homogeneously broadened lasers: higher-order bichromatic states," J. Opt. Soc. Am. B **2,** 211–217 (1985).
21. C. R. Stroud, Jr., K. Koch, and S. Chakmakjian, "Multimode instabilities in cw dye lasers," in *Optical Instabilities,* R. W. Boyd, M. G. Raymer, and L. M. Narducci, eds. (Cambridge U. Press, Cambridge, 1986), p. 47–50.
22. L. Allen and J. Eberly, *Optical Resonances and Two-Level Atoms* (Dover, New York, 1987).
23. E. T. Whittaker and G. N. Watson, *Modern Analysis* (Cambridge U. Press, Cambridge, 1965).
24. H. Risken and H. D. Vollmer, "Solutions and applications of tridiagonal vector recurrence relations," Z. Phys. B **39,** 339 (1980).
25. K. Koch, B. J. Oliver, S. H. Chakmakjian, and C. R. Stroud, Jr., "Subharmonic instabilites in resonant interactions with bichromatic fields," J. Opt. Soc. Am. B **6,** 58–65 (1989).
26. J. A. Abate, "Preparation of atomic sodium as a two-level atom," Opt. Commun. **10,** 269–272 (1974).
27. S. Kirkpatrick, C. D. Gelatt, Jr., and M. P. Vechi, "Optimization by simulated annealing," Science **220,** 671–680 (1983).
28. S. Kirkpatrick, "Optimization by stimulated annealing: quantitative studies," J. Stat. Phys. **34,** 975–986 (1984); C. C. Skiscim and B. L. Golden, "Optimization by stimulated annealing: a preliminary computational study for the TSP," in *Proceedings of the 1983 Winter Simulation Conference,* S. Roberts, J. Banks, and B. Schmeiser, eds. (Institute of Electrical and Electronics Engineers, New York, 1983), Vol. 1, pp. 523–535; M. E. Harrigan, "New approach to the optimization of lens systems," in *1980 International Lens Design Conference (Oakland),* R. E. Fischer, ed., Proc. Soc. Photo-Opt. Instrum. Eng. **237,** 66–74 (1980).